Reactions of 1,3-Cyclohexadiene with Singlet Oxygen. A Theoretical Study

Fatma Sevin[†,§] and Michael L. McKee*[,†]

Contributions from the Departments of Chemistry, Auburn University, Auburn, Alabama 36849, and Hacettepe University, Ankara, Turkey 06532

Received January 17, 2001. Revised Manuscript Received March 8, 2001

Abstract: A thorough study of the reaction of singlet oxygen with 1,3-cyclohexadiene has been made at the B3LYP/6-31G(d) and CASPT2(12e,10o) levels. The initial addition reaction follows a stepwise diradical pathway to form cyclohexadiene endoperoxide with an activation barrier of 6.5 kcal/mol (standard level = CASPT2(12e,10o)/6-31G(d); geometries and zero-point corrections at B3LYP/6-31G(d)), which is consistent with an experimental value of 5.5 kcal/mol. However, as the enthalpy of the transition structure for the second step is lower than the diradical intermediate, the reaction might also be viewed as a nonsynchronous concerted reaction. In fact, the concertedness of the reaction is temperature dependent since entropy differences create a free energy barrier for the second step of 1.8 kcal/mol at 298 K. There are two ene reactions; one is a concerted mechanism ($\Delta H^{\ddagger} = 8.8$ kcal/mol) to 1-hydroperoxy-2,5-cyclohexadiene (**5**), while the other, which forms 1-hydroperoxy-2,4-cyclohexadiene (**18**), passes through the same diradical intermediate (**9**) as found on the pathway to endoperoxide. The major pathway from the endoperoxide is O−O bond cleavage (22.0 kcal/mol barrier) to form a 1,4-diradical (**25**), which is 13.9 kcal/mol less stable than the endoperoxide. From the diradical, two low-energy pathways exist, one to epoxyketone (**29**) and the other to the diepoxide (**27**), where both products are known to be formed experimentally with a product ratio sensitive to the nature of substitutents. A significantly higher activation barrier leads to C−C bond cleavage and direct formation of maleic aldehyde plus ethylene.

Introduction

The reaction of singlet oxygen ($^1O_2$) with unsaturated olefins provides a valuable and convenient route to oxygen-functionalized products.[1] The major reaction pathway for cyclic conjugated dienes with singlet $^1O_2$ is 1,4-endoperoxides ([4π+2π adduct),[2] while acyclic conjugated dienes lead to endoperoxides, allylic hydroperoxides (ene reaction),[1d] and 1,2-dioxetanes ([2π+2π adduct) products with lack of stereospecificity as in the example of 2,5-dimethyl-2,4-hexadiene (Scheme 1).[3]

The ratio of these products depends on the structure of the diene and the reaction conditions, i.e., solvent and temperature.[4] For instance, the photooxidation products of α-terpinene (1-Me-4-*i*Pr-1,3-cyclohexadiene) are 90% endoperoxide and 5% diallyl hydroperoxides,[5] while α-phellandrene (2-Me-5-*i*Pr-1,3-cyclohexadiene) gives the endoperoxide and diallyl hydroperoxide products in a 65% to 32% ratio.[5] Also, formation of dioxetane is more favored in polar solvents than formation of the endoperoxide or ene reaction. The rate of reaction of 1,3-cyclohexadiene with $^1O_2$ is 10^2 times greater in methanol than in the gas phase ($\Delta H^{\ddagger} = 1.3$ kcal/mol in methanol and $\Delta H^{\ddagger} =$ 5.5 kcal/mol in the gas phase).[2a] This rate increase in a polar solvent versus gas phase is not observed for normal Diels-Alder reactions.[2a] Also of interest, the exothermicity of the photooxidation reaction to form the endoperoxide has been measured[2b] by using the photomicrocalorimetry technique in CCl_4 solvent to be −41.8 kcal/mol.

Scheme 1

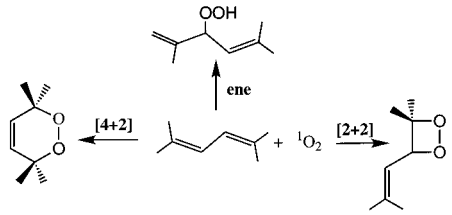

In recent work on acyclic dienes and olefin systems, Maranzana et al.,[6a] Yoshioka et al.,[6b] and Bobrowski et al.,[6c] have summarized the experimental and theoretical results on photooxidation mechanisms. Various reaction mechanisms for these

* Address correspondence to this author.
† Auburn University.
§ Hacettepe University.

(1) (a) Foote, C. S.; Clennan, E. L. In *Active Oxygen in Chemistry*; Foote, C. S.,; Valentine, J. S., Greenberg, A., Liebman, J. F., Eds.; Blackie Academic: New York, 1995; pp 105−140. (b) Bloodworth, A. J.; Eggelte, H. J. In *Singlet O_2, Reaction Modes and Products*; Frimer, A. A., Ed.; CRC Press: Boca Raton, FL, 1985; Vol. II, Part 1, pp 93−203. (c) Rigaudy, J. In Organic Photochemistry and Photobiology. *CRC Handbook*; Horspool, W. M., Song, P., Eds.; CRC Press: Boca Raton, FL, 1995; pp 325−334. (d) Griesbeck, A. G. In Organic Photochemistry and Photobiology. *CRC Handbook*; Horspool, W. M., Song, P., Eds.; CRC Press: Boca Raton, FL, 1995; pp 301−310. (e) Clennan, E. L.; Foote, C. S. In *Organic Peroxides*; Ando, W., Ed.; Wiley & Sons: Chichester, 1992; pp 253−318. (f) Kearns D. R. *Chem. Rev.* **1971**, *71*, 396−427. (g) Lissi, E. A.; Encinas, M. V.; Lemp, E.; Rubio, M. A. *Chem. Rev.* **1993**, *93*, 699−723.

(2) (a) Ashford, R. D.; Ogryzlo, E. A. *Can. J. Chem.* **1974**, *52*, 3544−3548. (b) Olmsted, J. *J. Am. Chem. Soc*. **1980**, *102*, 66−71. (c) Dumas, J. L. *Bull. Soc. Chim. Fr*. **1976**, *5*−*6*, 665−666.

(3) (a) Hasty, N. M.; Kearns, D. R. *J. Am. Chem. Soc*. **1973**, *95*, 3380−3381. (b) Manring, L. E.; Foote, C. S. *J. Am. Chem. Soc.* **1983**, *105*, 4710−4716.

(4) Gollnick, K.; Griesbeck, A. *Tetrahedron Lett.* **1984**, *25*, 725−728.

(5) Adam, W.; Griesbeck, A. G. In Organic Photochemistry and Photobiology. *CRC Handbook*; Horspool, W. M., Song, P., Eds.; CRC Press: Boca Raton, FL, 1995; pp 311−324.

10.1021/ja010138x CCC: $20.00
Published on Web 04/18/2001

Scheme 2

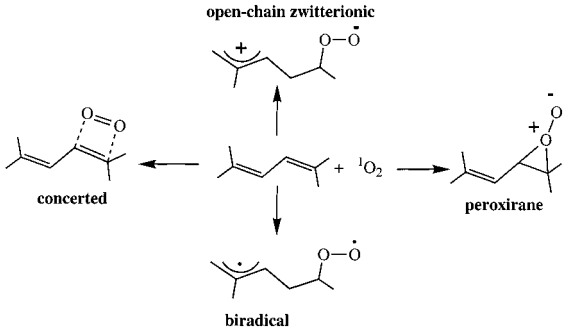

reactions have been proposed, which vary from concerted to nonconcerted and include diradical, open-chain zwitterionic, and/or peroxirane intermediates (Scheme 2).[7]However, the debate continues on the exact nature of the different mechanisms.

According to recent experimental results on conjugated diene systems, not only endoperoxide formation[8] but also the ene reaction and formation of 1,2-dioxetane can be explained by invoking the peroxirane intermediate or peroxirane-like exciplex.[9,10] Theoretical computations have been carried out to explore the ene, $2\pi+2\pi$, and $4\pi+2\pi$ reaction mechanisms with simple olefins and acyclic diene systems.[6] However, there is no theoretical study based on a cyclic diene system with $^1O_2$.

Predictions based on calculations change depending on the level of theory. At the semiempirical level[11] and the CASSCF level[12] that contain symmetry restrictions, it is concluded that peroxirane is the most probable intermediate. More recent studies[6a,b,13] without symmetry restrictions have not found the peroxirane intermediate to be important. For example, Maranzana et al. have suggested[6a] that the activation barrier for transformation of a diradical intermediate to peroxirane is higher than that for diradical closure to dioxetane. Also, the peroxirane pathway to dioxetane is prevented by a high-energy barrier, whereas the peroxirane can very easily collapse back to the diradical. In a study of the 1,4-cycloaddition of $^1O_2$ with *s-cis*-1,3-butadiene, Bobrowski et al.[6c] found a diradical intermediate on the lowest energy pathway (MCQDPT2/6-31G(d)) to endoperoxide. Thus these studies suggest a diradical intermediate in photooxidation reactions. A comparison of calculated relative energies for species on the potential energy surface for addition of O_2 to C_2H_4 and C_4H_6 is given in Table 1 along with present results for O_2 addition to C_6H_8 which will be discussed in greater detail below.

Table 1. Relative Energies (kcal/mol) for $^1O_2$ Addition to R = C_2H_4, C_4H_6, and C_6H_8 at Different Levels of Theory

	R = C_2H_4			R = C_4H_6		R = C_6H_8
	a	*b*	*c*	*s-trans*[a]	*s-cis*[d]	*e*
R + $^1O_2$	0.0			0.0	0.0	0.0
TS to diradical	17.5			11.7	4.7	6.5
diradical	8.3	0.0		−2.8	−3.6	−5.5
TS to dioxetane	16.4	6.7		8.8		4.0
dioxetane	−31.7	−43.5	0.0	−26.8		−29.8
TS for OO cleavage			19.5			−14.0
TS to endoperoxide					3.1	−5.9
concerted TS					7.7	16.7
endoperoxide					−52.0	−33.6

[a] Reference 6a. CASPT2(10e,10o)/6-31G(d)//CASSCF(12e,10o)/6-31G(d). [b] Reference 6b. CCSD(T)/6-31G(d)//MP2/6-31G(d). [c] Tanaka, C.; Tanaka, J. *J. Phys. Chem. A* **2000**, *104*, 2078−2090. CCSD(T)/6-31G(d)//B3LYP/6-31+G(d)+ZPC. [d] Reference 6c. MCQDPT2(10e,8o)/6-31G(d)//CASSCF(10e,8o)/6-31G(d). [e] This work. CASPT2(12e,10o)/6-31G(d)//B3LYP/6-31G(d)+ZPC.

While endoperoxides are products of singlet oxygen addition to conjugated dienes, they are also versatile starting materials for further transformations, due to homolytic cleavage of the O−O bond. The resulting diradicals are unstable and are rapidly transformed through intramolecular cyclization.[1,14] The photochemical reaction of cyclohexadiene endoperoxide gives *syn*-diepoxide and $\beta\gamma$-epoxycyclohexanone, which can be easily converted into the corresponding hydroxyenone by treatment with acids, bases, or silica gel, similar to that of thermolysis. In addition, the proportion of epoxyketone is larger from photolysis compared to thermolysis.[15] The diepoxide:epoxyketone product ratios in thermolysis and photolysis of cyclohexadiene endoperoxide are 35:65 and 28:72, respectively.[15] However, the actual transformation mechanism to form diepoxide and epoxyketone (and the nature of possible intermediates) is still unclear. Adam[14c] has suggested that the epoxyketone is a secondary product formed by rearrangement of diepoxide. Carless et al.[15] have suggested that a 1,3-diradical formed by closure of the first epoxide can either collapse to the diepoxide or rearrange by a hydrogen shift to an enol, which then tautomerizes to the ketone. Furthermore, the cleavage of one carbon bridge, subsequent or in concert with O−O homolysis, can lead to the epoxyaldehyde (Scheme 3). The latter is mainly obtained from saturated bicyclic endoperoxide by photolysis or thermolysis.[5,16]

Endoperoxides also undergo metal-promoted bimolecular decomposition, such as with CoTPP[17a,b] (cobalt (II) tetraphenylporphyrin) or $Pd(PPh_3)_4$.[17c] For example, Balci et al.[17d] have

(6) (a) Maranzana, A.; Ghigo, G.; Tonachini, G. *J. Am. Chem. Soc*. **2000**, *122*, 1414−1423. (b) Yoshioka, Y.; Tsunesada, T.; Yamaguchi, K.; Saito, I. *Int. J. Quantum Chem.* **1997**, *65*, 787−801. (c) Bobrowski, M.; Liwo, A.; Ołdziej, S.; Jeziorek, D.; Ossowski, T. *J. Am. Chem. Soc*. **2000**, *122*, 8112−8119.

(7) For an interesting report on trapping zwitterionic peroxide intermediates see: Jefford, C. W. *Chem. Soc. Rev.* **1993**, 59−66.

(8) (a) Clennan E. L.; Mehrsheikh-Mohammadi, M. E. *J. Am. Chem. Soc*. **1984**, *106*, 7112−7118. (b) Clennan, E. L.; Mehrsheikh-Mohammadi, M. E. *J. Org. Chem.* **1984**, *49*, 1321−1322. (c) Monroe, B. M *J. Am. Chem. Soc*. **1981**, *103*, 7253−7256. (d) Aubry, J.-M.; Mandard-Cazin, B.; Rougee, M.; Bensasson, R. V. *J. Am. Chem. Soc.* **1995**, *117*, 9159−9164.

(9) (a) Manring, L. E.; Foote, C. S. *J. Am. Chem. Soc*. **1983**, *105*, 4710−4717. (b) Poon, T. H. W.; Pringle, K.; Foote, C. S. *J. Am. Chem. Soc*. **1993**, *117*, 7611−7618. (c) Vassilikogiannakis, G.; Stratakis, M.; Orfanopoulus, M. *J. Org. Chem.* **1998**, *63*, 6390−6393. (d) Harding, L. B.; Goddard, W. A. *J. Am. Chem. Soc.* **1980**, *102*, 439−449. (e) Harding, L. B.; Goddard, W. A. *Tetrahedron Lett.* **1978**, 747−750.

(10) Clennan, E. L. *Tetrahedron* **2000**, *56*, 9151−9179.

(11) (a) Inagaki, S.; Yamabe, S.; Fujimoto, H.; Fukui, K. *Bull. Chem. Soc. Jpn.* **1972**, *45*, 3510−3514. (b) Inagaki, S.; Fukui, K. *J. Am. Chem. Soc.* **1975**, *97*, 7480−7484. (c) Dewar, M. J. S. *Chem. Br.* **1975**, *11*, 97−106. (d) Dewar, M. J. S. *J. Am. Chem. Soc.* **1975**, *97*, 3978−3986. (e) Dewar, M. J. S.; Griffin, A. C.; Thiel, W.; Turchi, I. J. *J. Am. Chem. Soc.* **1975**, *97*, 4439−4440. (f) Yamaguchi, K.; Yabushita, S.; Fueno, T.; Houk, K. N. *J. Am. Chem. Soc.* **1981**, *103*, 5043−5046. (g) Davis, K. M.; Carpenter, B. K. *J. Org. Chem.* **1996**, *61*, 4617−4622.

(12) Hotokka, M.; Roos, B.; Siegbahn, P. J. *J. Am. Chem. Soc*. **1983**, *105*, 5263−5269.

(13) (a) Tonachini, G.; Schlegel, H. B.; Bernardi, F.; Robb, M. A. *THEOCHEM* **1986**, *138*, 221−227. (b) Tonachini, G.; Schlegel, H. B.; Bernardi, F.; Robb, M. A. *J. Am. Chem. Soc.* **1990**, *112*, 483−491. (c) Liwo, A.; Dyl, D.; Jeziorek, D.; Nowacka, M.; Ossowski, T.; Woźnicki, W. *J. Comput. Chem.* **1997**, *18*, 1668−1681.

(14) (a) Adam, W.; Balci, M. *Tetrahedron* **1980**, *36*, 833−858. (b) Balci, M. *Chem. Rev.* **1981**, *81*, 91−108. (c) Adam, W. *Angew. Chem., Int. Ed. Engl.* **1974**, *13*, 619−628.

(15) Carless, H. A. J.; Atkins, R.; Fekarurhobo, G. K. *Tetrahedron Lett.* **1985**, *26*, 803−806.

(16) Bloodworth, A. J.; Eggelte, H. J. *Tetrahedron Lett.* **1984**, *25*, 1525−1528.

(17) (a) Balci, M.; Sütbeyaz, Y. *Tetrahedron Lett.* **1983**, *24*, 4135−4140. (b) Balci, M.; Akbulut, N. *Tetrahedron* **1985**, *41*, 1315−1322. (c) Suzuki, M.; Oda, Y.; Noyori, R. *Tetrahedron Lett*. **1981**, *44*, 4413−4416. (d) Balci M.; Kilic, H.; Adam, W.; *J. Org. Chem*. **2000**, *65*, 5926−5931. (e) Özer, G.; Saraçoğlu, N.; Balci, M. *Heterocycles* **2000**, *53*, 761−764.

Scheme 3

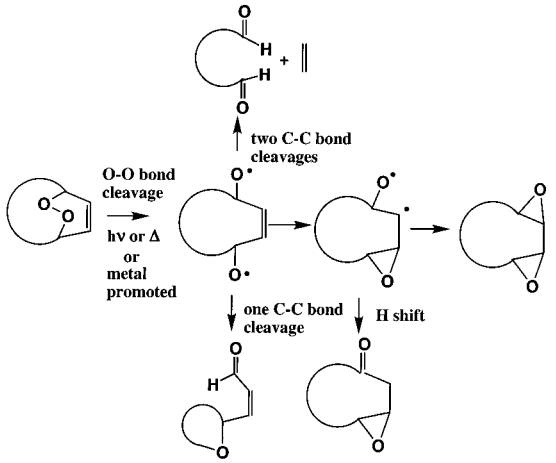

obtained *syn*-diepoxyhexanone, maleic aldehyde, and 4,6-epoxyhexenal in a 50:32:18 ratio, respectively, from the rearrangement of unsaturated endoperoxide ketone with CoTPP by thermolysis. The mechanism of product formation is rationalized by invoking β-scission of either a one- or two-carbon bridge in an alkoxy radical formed by inner-sphere electron transfer from CoTPP to the peroxide linkage.[17] In some cases, the formation of epoxyketone is not observed, but rather open-chain aldehydes are encountered by CoTPP-catalyzed decomposition of endoperoxide derivatives, such as cycloheptatriene endoperoxide[18] and 8,9-dioxatricyclo[5.2.2.0]undec-10-en-4-one.[17b] To explain the absence of the epoxyketone product in CoTPP-catalyzed reactions of endoperoxides, it has been assumed[18a] that the activation energy for the 1,2-hydrogen shift is higher than that for diepoxide formation, and that CoTPP cleaves the oxygen−oxygen bond by an electron-transfer mechanism at a temperature too low (−10 °C) for hydrogen transfer to occur.

The photochemical reactions of endoperoxides have also attracted attention.[19−22] Very recently, both theoretical (INDO/S and CNDO/S) and experimental studies of the electronic states of aromatic endoperoxides by Klein et al.[19] and Kearns[20] have rekindled the controversy involving the dual photochemistry of the endoperoxide (i.e. different product formation with different light wavelength). According to Kearns,[20] who made his predictions using state and orbital correlation diagrams of cyclopentadiene endoperoxide, the O−O bond cleavage to produce the endoperoxide diradical takes place from the first excited singlet state ($\pi^*_{OO} \rightarrow \sigma^*_{OO}$), while the cycloreversion to produce diene and singlet oxygen occurs from the second excited state of endoperoxide with electronic excitation ($\pi^*_{OO} \rightarrow \sigma^*_{CO}$).

Furthermore, Rigaudy et al.[22] reported the first observation of wavelength-dependent product distribution of 9,10-diphenylanthracene endoperoxide. Several picosecond time-resolved studies followed which demonstrated that photocycloreversion

Scheme 4

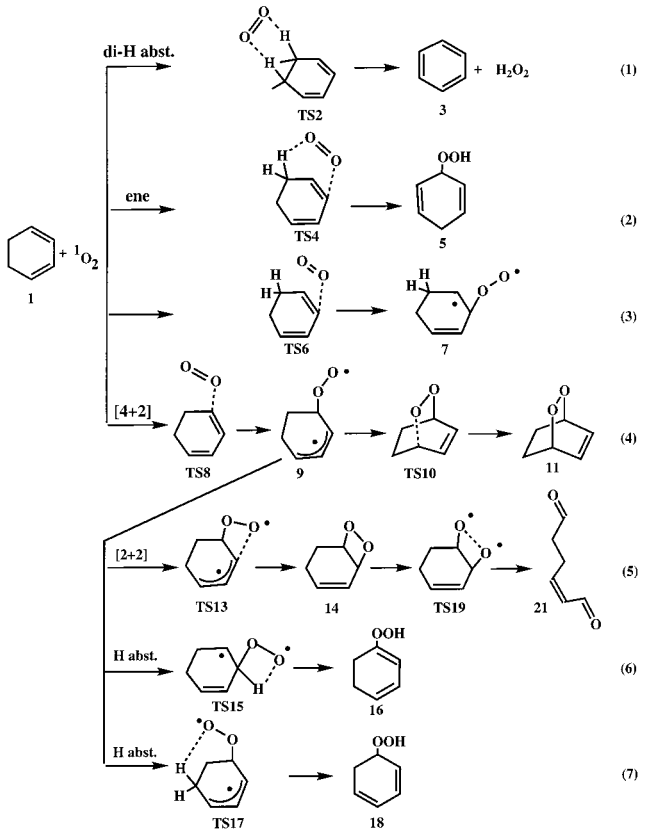

of endoperoxides occurs from higher excited singlet states (S_n, $n \geq 2$) in nonconcerted fashion with a barrier in the last step of reaction.[22] In the most recent paper, and in contrast to all previous results, Klein et al.[19] have suggested, based on the spectroscopic behavior of aromatic endoperoxides, that cycloreversion of anthracene 9,10-endoperoxide and of 9,10-dimethylanthracene-9,10-endoperoxide takes place from the lowest S_1 state ($\pi-\pi^*$ excitation from ground state). Thus it is desirable to calculate both the singlet and triplet excited states to assess their nature.

Finally, as mentioned above, not only possible photooxidation reactions with 1,3-cyclohexadiene of singlet oxygen (Scheme 4) but also the O−O bond cleavage with one and two C−C bond cleavage reactions from the endoperoxide (Scheme 5) have not been previously studied theoretically. From the mechanistic point of view, the situation is still complicated since the same products may be formed from different pathways as well as via concerted or stepwise mechanisms. From this perspective, it seems worthwhile to study the energetics by reliable theoretical methods to test their predictive powers at a consistent level of theory.

Computational Methods

The photooxidation reactions of 1,3-cyclohexadiene by singlet oxygen considered in the present study are given in Scheme 4 and Scheme 5. Two different theoretical approaches were used in this work. First, density functional theory at the B3LYP/6-31G(d)[23] level was used to optimize all stationary points. Vibrational frequencies were calculated analytically for all optimized structures to determine the nature of stationary points and to obtain zero-point and heat capacity corrections.

Many of the intermediates in this study can be characterized as diradicals and most of the species have significant contributions from

(18) (a) Sütbeyaz, Y.; Seçen, H.; Balci, M. *J. Org. Chem.* **1988**, *53*, 2312−2317. (b) Sengul, M. N.; Simsek, N.; Balci, M. *Eur. J. Org. Chem.* **2000**, 1359−1363.

(19) (a) Klein, A.; Kalb, M.; Gudipati, M. S. *J. Phys. Chem. A.* **1999**, *103*, 3843−3853. (b) Gudipati, M. S.; Klein, A. *J. Phys. Chem. A* **2000**, *104*, 166−167.

(20) (a) Kearns, D. R. *J. Am. Chem. Soc.* **1969**, *91*, 6554−6560. (b) Kearns, D. R.; Khan, A. U. *Photochem. Photobiol.* **1969**, *10*, 193-210.

(21) (a) Schmidt, R.; Schaffner, K.; Brauer, H.-D. *J. Phys. Chem.* **1984**, *88*, 956−958. (b) Brauer, H.-D.; Schmidt, R. *J. Phys. Chem. A* **2000**, *104*, 164−165.

(22) Rigaudy, J.; Breliere, C.; Scribe, P. *Tetrahedron Lett.* **1978**, *28*, 687−692.

(23) (a) Becke, A. D. *J. Chem. Phys.* **1993**, *98*, 5648−5652. (b) Lee, C.; Yang, W.; Parr, R. G. *Phys. Rev. B* **1988**, *37*, 785−789.

Scheme 5

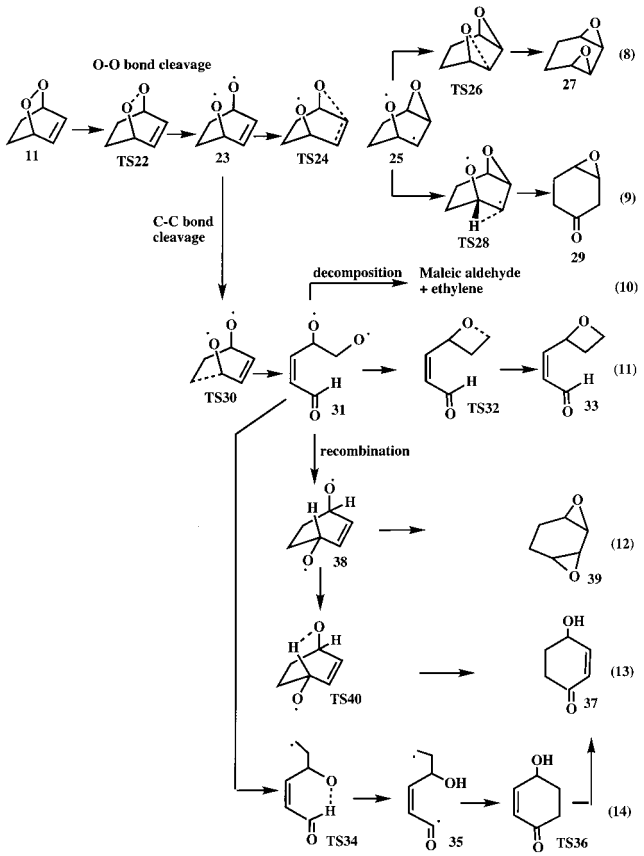

more than one configuration. A popular approach[24] (but not one above reproach[25]) is to optimize geometries with an unrestricted DFT method (UDFT) where the α and β electrons are allowed to de-couple. A disadvantage to this method is that the spin-squared value (which should be 0.0 for a singlet) often approaches 1.0 for a strong diradical. Nevertheless, many studies have reported good success with results that closely match those of more rigorous methods. Our approach is to find the "broken-symmetry" open-shell solution whenever possible and to use this geometry for higher level calculations.

On fixed geometries, CASPT2 calculations were carried out to include the effects of nondynamic and dynamic electron correlation.[26] For the dioxygen molecule, an active space was chosen to include 8-electrons in 6-orbitals (8e,6o). The same active space was used for hydrogen peroxide and maleic aldehyde. For benzene and cyclohexadiene, a 4-electrons in 4-orbitals (4e,4o) space was used, while for all $C_6H_8O_2$ species, a 12-electrons in 10-orbitals (12e,10o) active space was used. The default correction to the Fock matrix (G0) was used in all CASPT2 calculations. All CASSCF and CASPT2 calculations were made without symmetry constraints on the wave function.

In Table 2, the CASPT2 natural orbital occupation numbers of the HOMO and LUMO (the two orbital occupations which differ most from 2.0 and 0.0) are compared with $\langle S^2 \rangle$ values at the UB3LYP/6-31G(d) level. In general, there is a good correlation between the HOMO or LUMO orbital population and $\langle S^2 \rangle$. At the onset of symmetry breaking, where the unrestricted DFT solution is lower in energy than the restricted solution, the CASPT2 HOMO orbital population is about 1.7 electrons and the LUMO population is about 0.2 electrons. As the $\langle S^2 \rangle$ values increase to that of a diradical ($\langle S^2 \rangle = 1.00$), the HOMO and LUMO populations approach 1.0 electron (Figure 1).

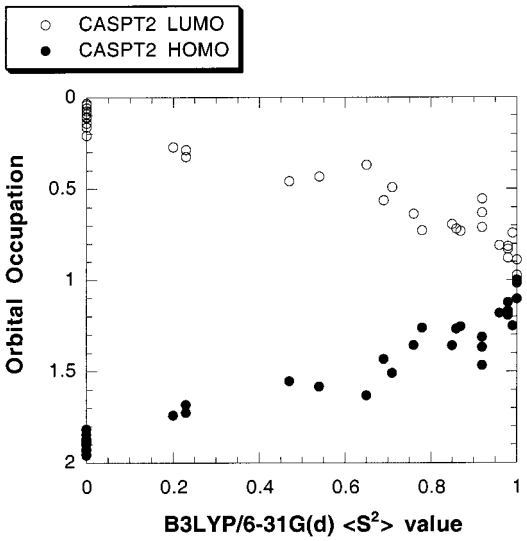

Figure 1. Plot of HOMO and LUMO populations at the CASPT2-(12e,10o)/6-31G(d) level versus the $\langle S^2 \rangle$ value calculated at the B3LYP/6-31G(d) level.

For two structures, **9** and **TS17**, both closed-shell geometries (**9clo** and **TS17clo**) and open-shell geometries (**9opn**, $\langle S^2 \rangle = 0.98$, and **TS17opn**, $\langle S^2 \rangle = 0.47$) were calculated. At the UB3LYP/6-31G(d)+ZPC level, the open-shell energies were 16.1 and 3.5 kcal/mol lower than the closed-shell geometries for **9** and **TS17**, respectively. At the CASPT2+ZPC level, the open-shell UDFT (spin-unrestricted DFT) geometries produced lower energies (by 4.6 and 0.8 kcal/mol) than the RDFT (spin-restricted DFT) closed-shell geometries for **9** and **TS17**, respectively. Thus we feel that open-shell geometries, obtained at the UB3LYP/6-31G(d) level, are the more appropriate ones to use for single-point CASPT2 calculations.

The imaginary frequencies (transition vectors) were animated graphically for all transition structures to ensure that the motions were appropriate for converting reactants to products.[27] It should be noted that several transition structures (i.e. **TS6** and **TS8**) may lead to local conformational minima. However, small rotational (or conformational) barriers (not calculated) should lead to the intermediate given the reaction profile diagram (i.e. an IRC from **TS6** (**TS8**) may not lead directly to **7** (**9**) but rather to a related conformatiuonal minimum).

The calculated relative energies, enthalpies (0 K), and free energies (298 K) relative to 1,3-cyclohexadiene (**1**) + singlet oxygen ($^1O_2$) are presented in Table 2. The relative energies in the reaction profiles in Figures 2−6 were calculated at the standard level of CASPT2(12e,10o)/6-31G(d)//B3LYP/6-31G(d)+ZPC. At the standard level, the $^1\Delta_g - \Sigma_g^{3+}$) splitting in molecular oxygen is calculated to be 24.7 kcal/mol, in fair agreement with the experimental value of 22.5 kcal/mol.[1g] At the UB3LYP/6-31G(d) level, the splitting is calculated to be much too small (10.4 kcal/mol). Therefore, comparisons in Table 2 at the DFT level will be relative to 1,3-cyclohexadiene plus $^3O_2$, which will be assigned a value of −22.5 kcal/mol.[28] While the CASPT2 energies are more reliable, the agreement between the two methods in Table 2 is, in general, quite good. However, it should be noted that the 6-31G(d) basis set may not be sufficiently flexible to produce reliable energetics across the entire potential energy surface.[29]

(24) (a) Goldstein, E.; Beno, B.; Houk, K. N. *J. Am. Chem. Soc.* **1996**, *118*, 6036−6043. (b) Cramer, C. J. *J. Am. Chem. Soc.* **1998**, *120*, 6261−6269. (c) Gräfenstein, J.; Cremer, D. *Chem. Phys. Lett.* **1998**, *288*, 593−602. (d) Koch, W.; Holthausen, M. C. *A Chemist's Guide to Density Functional Theory*; Wiley-VCH: Weinheim, 2000.

(25) Jarzęcki, A. A.; Davidson, E. R. *J. Phys. Chem. A* **1998**, *102*, 4742−4746.

(26) Andersson, K.; Roos, B. O. *Int. J. Quantum Chem.* **1993**, *45*, 591−607.

(27) MOLDEN: Schaftenaar G.; Noordik, J. H. Molden: a pre- and post-processing program for molecular and electronic structures. *J. Comput.-Aided Mol. Design* **2000**, *14*, 123−134.

(28) No "energy decontamination" procedure has been used to compensate for the effect of spin contamination in the B3LYP/6-31G(d) energies.

(29) A point of contact between theory and experiment is the reaction enthalpy for C_6H_8 (**1**) + $^3O_2 \rightarrow C_6H_6$ (**3**) + H_2O_2, which is −37.7 kcal/mol at 298K [NIST Chemistry Webbook; http://webbook.nist.gov/chemistry]. At the B3LYP/6-31G(d)+ZPC or CASPT2/6-31G(d)//B3LYP/6-31G(d)+ZPC levels, the values are too small (−26.7 and −25.4 kcal/mol, respectively). The agreement with experiment improves at the B3LYP/6-31+G(d,p)//B3LYP/6-31G(d)+ZPC level (−36.6 kcal/mol).

Table 2. Relative Energies (kcal/mol) of Species on the $C_6H_8O_2$ Potential Energy Surface

	B3LYP/ 6-31G(d)[a]	$\langle S^2\rangle$[b]	B3LYP/ 6-31G(d)+ZPC[a]	CASPT2/ 6-31G(d)[c]	orbital population[d] HOMO	orbital population[d] LUMO	CASPT2/ 6-31G(d)+ZPC[c]	ΔG(298K)[e]
1 + $^1O_2$	0.0[−12.1]	1.00	0.0[−12.1]	0.0			0.0	0.0
1 + $^3O_2$	−22.5	2.01	−22.5	−24.7			−24.7	−25.3
TS2	15.3	0.0	13.3	24.2	1.845	0.162	22.1	31.2
3 + H_2O_2	−49.4	0.0	−49.2	−50.4			−50.1	−50.3
TS4	8.7	0.0	9.3	8.2	1.815	0.208	8.8	16.4
5	−33.9	0.0	−31.7	−34.1	1.900	0.089	−31.9	−22.9
TS6	7.6	0.92	7.8	11.4	1.467	0.554	11.5	20.6
7	5.8	0.92	6.8	9.7	1.312	0.711	10.7	19.5
TS8	−1.7	1.05	−1.4	6.2	1.096	0.948	6.5	15.2
9opn	−9.2	0.98	−7.8	−7.0	1.195	0.816	−5.5	2.7
9clo	6.8	0.0	9.0	−2.3	1.423	0.592	−0.2	9.3
TS10	−5.2	0.54	−3.2	−7.9	1.582	0.433	−5.9	4.5
11	−39.5	0.0	−35.4	−37.6	1.899	0.090	−33.6	−23.1
12	8.5	0.0	9.5	15.6	1.869	0.141	16.7	26.2
TS13	1.7	0.65	3.1	2.7	1.630	0.370	4.0	13.9
14	−33.3	0.0	−29.4	−33.6	1.901	0.089	−29.8	−19.9
TS15	21.3	0.52	20.0	20.2	1.578	0.418	19.0	28.5
16	−38.4	0.0	−36.2	−31.9	1.922	0.075	−29.7	−20.6
TS17opn	5.2	0.47	4.4	5.5	1.553	0.457	4.8	15.1
TS17clo	8.6	0.0	9.0	6.3			6.7	17.0
18	−34.0	0.0	−31.8	−33.2	1.883	0.110	−30.9	−21.8
TS19	−10.9	0.82	−9.2	−15.6	1.530	0.461	−14.0	−4.0
20	−91.9	0.0	−90.7	−87.6	1.885	0.113	−86.3	−78.8
21	−92.7	0.0	−92.1	−89.9	1.900	0.092	−89.3	−80.7
TS22	−12.3	0.92	−11.3	−14.1	1.368	0.631	−13.1	−3.1
23	−20.9	1.00	−19.7	−19.1	1.017	0.974	−17.8	−8.3
TS24	−16.2	0.96	−15.8	−12.0	1.181	0.810	−11.6	−1.7
25	−20.6	0.76	−20.1	−20.2	1.356	0.636	−19.7	−10.0
TS26	−19.2	0.85	−18.2	−17.6	1.358	0.636	−16.6	−6.5
27	−69.6	0.0	−65.3	−66.8	1.953	0.041	−62.5	−52.2
TS28	−20.6	0.69	−20.5	−20.4	1.432	0.563	−20.4	−10.4
29	−99.8	0.0	−96.0	−99.9	1.935	0.057	−96.0	−86.6
TS30	−4.8	0.99	−6.0	0.0	1.251	0.741	−1.2	7.9
male + eth[f]	−69.9	0.0	−72.3	−63.4			−65.8	−68.4
31	−17.7	0.78	−19.2	−11.3	1.262	0.728	−12.8	−4.3
TS32	−12.9	0.86	−14.7	−8.4	1.269	0.719	−10.2	−2.6
33	−75.3	0.0	−72.9	−69.4	1.892	0.106	−67.0	−58.7
TS34	−15.5	0.98	−20.2	−6.6	1.122	0.878	−11.3	−3.4
35	−28.5	1.00	−30.4	−27.0	1.105	0.890	−28.9	−23.3
TS36	−27.9	1.01	−30.1	−24.7	1.092	0.898	−26.8	−18.8
37	−105.8	0.0	−102.2	−105.8	1.896	0.112	−102.2	−92.8
38	−20.5	1.00	−19.7	−16.7	1.003	0.984	−16.0	−6.0
39	−73.8	0.0	−69.4	−70.7	1.952	0.042	−66.3	−55.5
TS40	−12.8	0.87	−13.5	−13.0	1.256	0.731	−13.7	−3.5
TS41	−13.8	0.71	−12.7	−26.9	1.509	0.491	−25.9	−15.7
42	−30.3	0.23	−27.8	−39.9	1.725	0.287	−37.3	−27.4
TS43	−23.8	0.23	−21.6	−34.3	1.681	0.324	−32.1	−22.0
44	−31.3	0.20	−29.0	−37.0	1.741	0.273	−34.7	−24.8
TS45	−13.1	0.98	−12.1	−20.6	1.170	0.830	−19.6	−9.7
46	−70.5	0.0	−66.3	−66.8	1.953	0.041	−62.6	−52.0
TS47	−14.0	1.00	−13.3	−15.5	1.001	0.998	−14.8	−4.9

[a] The value in brackets is the calculated relative energy of $^1O_2$. All entries in this column are with respect to $^3O_2$ which is assigned a value of −22.5 kcal/mol, the experimental S−T splitting of O_2. [b] Spin-squared value at the UB3LYP/6-31G(d) level before spin projection. [c] CASPT2(12e,10o)/6-31G(d). [d] Natural orbital population for the two orbitals which deviate most from 2.0 (HOMO) and 0.0 (LUMO). [e] Heat capacity corrections and entropies computed at the B3LYP/6-31G(d) level at 298 K are used with relative energies at the CASPT2(12e,10o)/6-31G(d)//B3LYP/6-31G(d)+ZPC level to compute free energies. [f] Maleic aldehyde plus ethylene.

The CASSCF and CASPT2 calculations were made with the MOLCAS 4.1[30] program and the DFT calculations were carried out with GAUSSIAN98.[31] Total energies, zero-point energies, thermodynamic parameters, and Cartesian coordinates of B3LYP/6-31G(d) optimized structures are available as Supporting Information. Vertical electronic excitation energies for cyclohexadiene and cyclopentadiene endoperoxides were calculated by using the TD-B3LYP method[32] based on B3LYP/6-31+G(d) optimized ground-state geometries.

(30) Andersson, K.; Blomberg, M. R. A.; Fülscher, M. P.; Karlström, G.; Lindh, R.; Malmqvist, P.-Å.; Neogrády, P.; Olsen, J.; Roos, B. O.; Sadlej, A. J.; Schütz, M.; Seijo, L.; Serrano-Andrés, L.; Siegbahn, P. E. M.; Widmark, P.-O. *MOLCAS*, version 4.1; Lund University, Sweden, 1997.

Results and Discussion

Reactions of 1,3-Cyclohexadiene with $^1O_2$. The only product of singlet oxygen ($^1O_2$) plus 1,3-cyclohexadiene (**1**) is endoperoxide.[4] However, in the reaction of singlet oxygen with cyclic dienes where the cis form of diene is inaccessible and/or the ionization potential of olefin is lowered by terminal alkyl substitution, the reaction pathway is diverted to one that resembles the reaction of monoolefins with $^1O_2$. For that reason, various possibilities have been examined in the present study.

One unusual pathway is the formation of benzene and hydrogen peroxide, which might be formed by a concerted dihydrogen abstraction in eq 1 (Scheme 4). A similar concerted

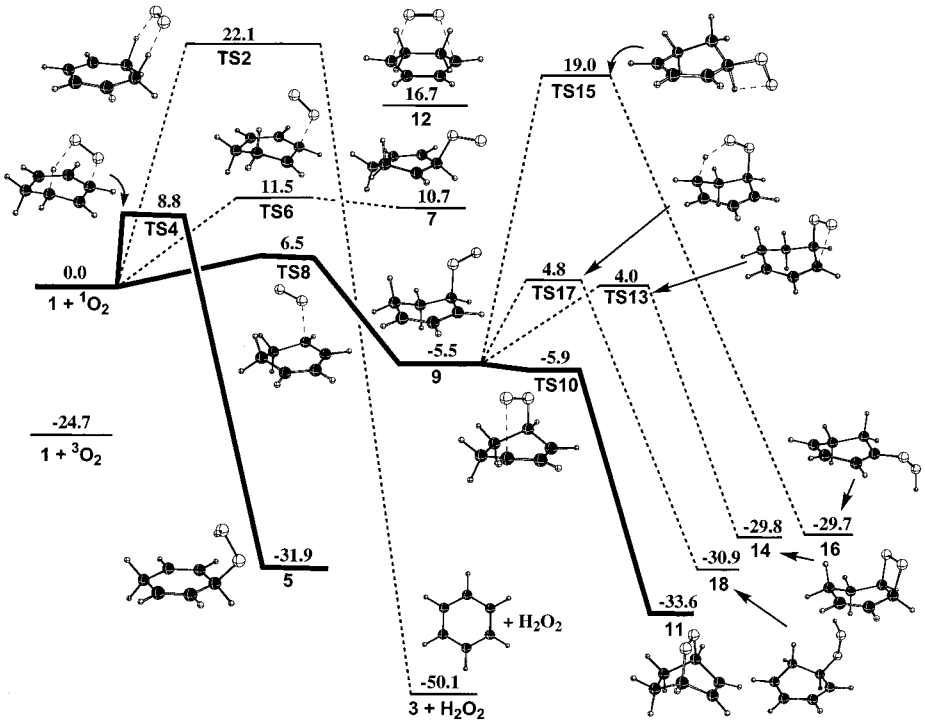

Figure 2. Reaction diagram (kcal/mol) of $C_6H_8O_2$ species calculated at the CASPT2/6-31G(d)//B3LYP/6-31G(d)+ZPC level starting from 1,3-cyclohexadiene (**1**) plus $^1O_2$.

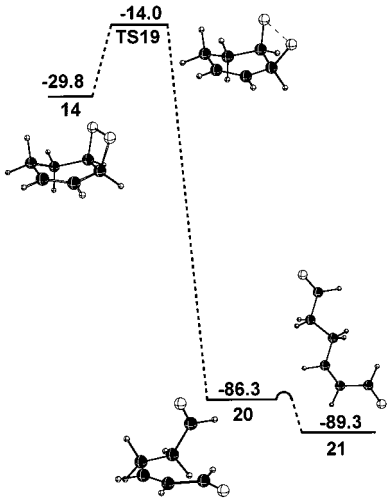

Figure 3. Reaction diagram (kcal/mol) of $C_6H_8O_2$ species calculated at the CASPT2/6-31G(d)//B3LYP/6-31G(d)+ZPC level starting from the dioxetane (**14**).

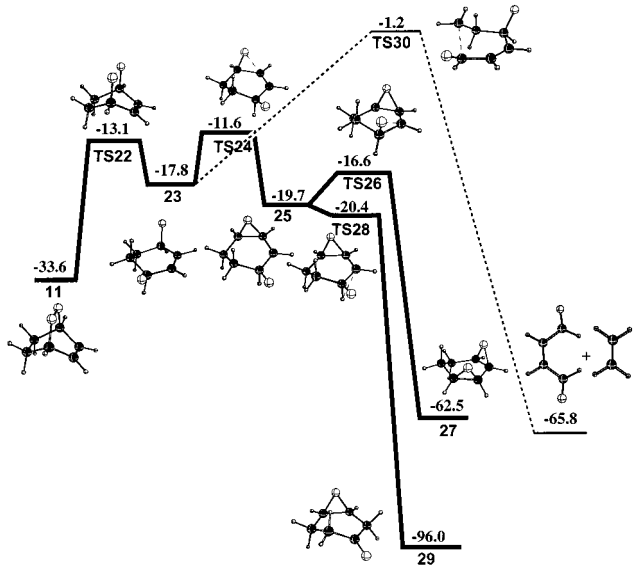

Figure 4. Reaction diagram (kcal/mol) of $C_6H_8O_2$ species calculated at the CASPT2/6-31G(d)//B3LYP/6-31G(d)+ZPC level starting from endoperoxide (**11**).

reaction mechanism has recently[33] been calculated at the CCSD(T)/6-311G(d,p)//B3LYP/6-31G(d,p)+ZPC level for the reaction of singlet oxygen with hydroxymethylformate to form formic acid anhydride plus H_2O_2. In this system, one O−H and one C−H hydrogen are abstracted. The calculated barrier (22.7 kcal/mol) is quite similar to the 22.1 kcal/mol barrier calculated here for **1** + $^1O_2$ → **TS2**.

The lowest energy barrier is for formation of endoperoxide in a two-step process (eq 4, Scheme 4) where the first step has an activation barrier of 6.5 kcal/mol (**TS8**) at the CASPT2 level, which is close to the experimental value of 5.5 ± 2 kcal/mol in the gas phase.[2a] **TS8** has reactant-like character and the C−O and O═O bond distances are 1.947 and 1.266 Å (the calculated bond distance of $^1O_2$ is 1.215 Å). The intermediate **9** is 5.5

(31) Frisch, M. J.; Trucks, G. W.; Schlegel, H. B.; Scuseria, G. E.; Robb, M. A.; Cheeseman, J. R.; Zakrzewski, V. G.; Montgomery, J. A., Jr.; Stratmann, R. E.; Burant, J. C.; Dapprich, S.; Millam, J. M.; Daniels, A. D.; Kudin, K. N.; Strain, M. C.; Farkas, O.; Tomasi, J.; Barone, V.; Cossi, M.; Cammi, R.; Mennucci, B.; Pomelli, C.; Adamo, C.; Clifford, S.; Ochterski, J.; Petersson, G. A.; Ayala, P. Y.; Cui, Q.; Morokuma, K.; Malick, D. K.; Rabuck, A. D.; Raghavachari, K.; Foresman, J. B.; Cioslowski, J.; Ortiz, J. V.; Stefanov, B. B.; Liu, G.; Liashenko, A.; Piskorz, P.; Komaromi, I.; Gomperts, R.; Martin, R. L.; Fox, D. J.; Keith, T.; Al-Laham, M. A.; Peng, C. Y.; Nanayakkara, A.; Gonzalez, C.; Challacombe, M.; Gill, P. M. W.; Johnson, B. G.; Chen, W.; Wong, M. W.; Andres, J. L.; Head-Gordon, M.; Replogle, E. S.; Pople, J. A. *Gaussian 98*, Gaussian, Inc.: Pittsburgh, PA, 1998.

(32) van Gisbergen, J. A.; Kootstra, F.; Schipper, R. P. T.; Gritsenko, O. V.; Snijders, J. G.; Baerends, E. J. *Phys. Rev. A* **1998**, *57*, 2556−2571 and references therein.

(33) Aplincourt, P.; Ruiz-López, M. F. *J. Phys. Chem. A* **2000**, *104*, 380−388.

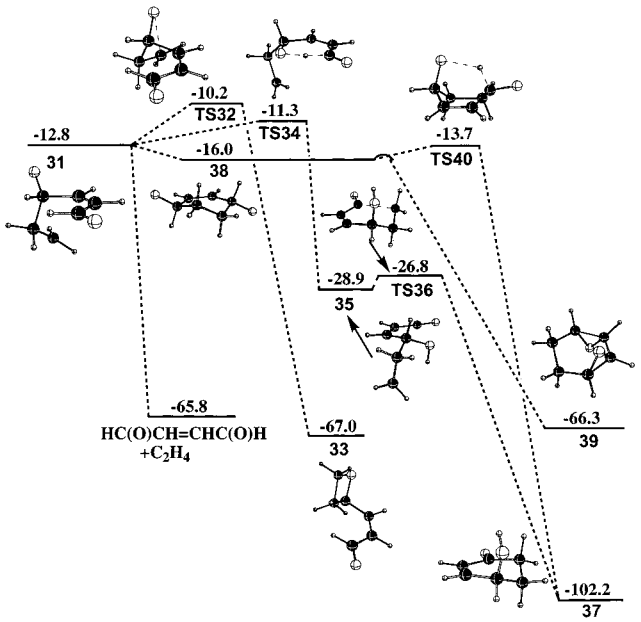

Figure 5. Reaction diagram (kcal/mol) of $C_6H_8O_2$ species calculated at the CASPT2/6-31G(d)//B3LYP/6-31G(d)+ZPC level starting from acyclic diradical (**31**).

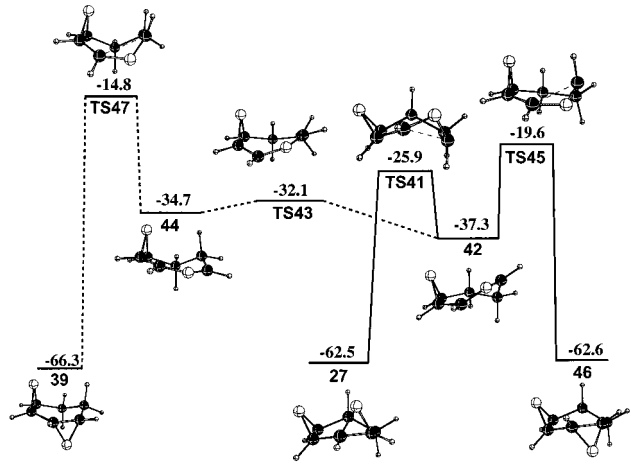

Figure 6. Reaction diagram (kcal/mol) for conversion of *syn*-diepoxide (**27**) to *anti*-diepoxide (**39**).

kcal/mol more stable than reactants while the second barrier (**TS10**) is 0.4 kcal/mol *below* intermediate **9**.

The experimental observation that the activation barrier for endoperoxide formation is lower in polar solvents than in the gas phase can be explained by the polar nature of **TS8**. At the B3LYP/6-31G(d) level, the dipole moment of **TS8** is 2.89 D due to the transfer of 0.26 electron from cyclohexadiene to O_2. By contract, the dipole moment of the reactant cyclohexadiene is only 0.38 D. The effect of solvation on the intermediate **9** (D.M. = 3.34 D) and second transition structure **TS10** (D.M. = 3.13 D) should be similar to that of **TS8**.

The structure of intermediate **9** is interesting in that it might have diradical or zwitterionic character. The charge distribution of **9** is consistent with three important resonance structures (RS) which can be called exciplex, diradical, and zwitterionic (Figure 7). The UDFT geometry (**9opn**) has less contribution from the zwitterionic RS as seen from the summed charges (0.08 e) on the CH units labeled "b" compared to the summed charges (0.17 e) for "b" in the RDFT geometry (**9clo**). In addition, the CASPT2 natural HOMO/LUMO population for **9opn** and **9clo** (1.195/0.816 vs 1.423/0.592, Table 2) also indicates greater

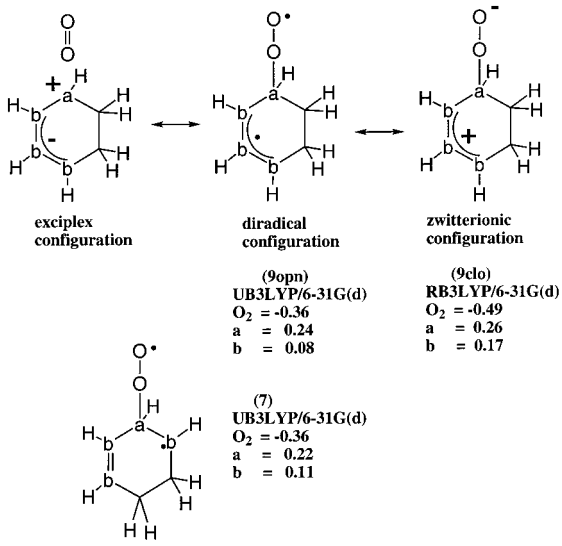

Figure 7. Illustration of the contributing resonance structures to the O_2-adducts **9opn**, **9clo**, and **7**. Mulliken populations at UB3LYP/6-31G(d) refer to the **9opn** and **7** geometries, while the RB3LYP/6-31G(d) values refers to the **9clo** geometry.

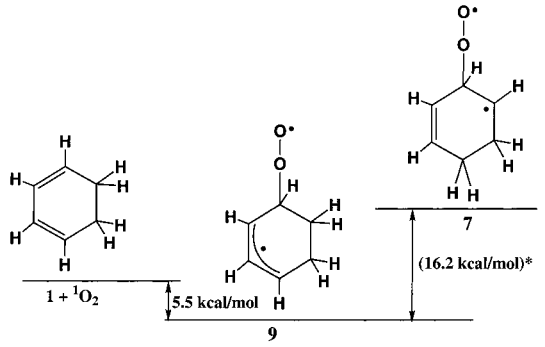

Figure 8. One unpaired electron in **9** is delocalized over three carbon atoms while an unpaired electron is localized on one carbon in **7**. The energy difference between the two adducts (16.2 kcal/mol) is close to the known allylic resonance energy[35] (15.7 ± 1 kcal/mol).

diradical character for the geometry of **9opn**. The exciplex RS arises from internal excitation of cyclohexdiene, which places a positive charge on the carbon that binds to O_2. A significant degree of charge transfer to O_2 also takes place upon binding (−0.36 e for **9opn** and −0.49 e for **9clo**).

A similar contribution of resonance structures can be noted for **7**, which is another O_2 adduct of cyclohexadiene. The difference between **7** and **9** is that an unpaired electron is localized on one carbon center in **7**, while it is delocalized over three carbon centers in **9** (Figure 8). In fact, the energy difference between **7** and **9** (16.2 kcal/mol) corresponds closely to the experimental conjugative stabilization energy (CSE) of the allylic radical (15.7 ± 1 kcal/mol).[34] Harding and Goddard[9d] have noted that O_2 prefers to attack the terminal CH_2 of butadiene because it creates a delocalized allylic system.

The entropy of activation has been measured for the addition of $^1O_2$ to cyclopentadiene (−25.8 cal/(mol·K)).[35] Our calculated value for the addition of $^1O_2$ to cyclohexadiene is similar (−31.2 cal/(mol·K)), which might be indicative of a similar mechanism.

(34) Korth, H.-G.; Trill, H.; Sustmann, R. *J. Am. Chem. Soc.* **1981**, *103*, 4483−4489.

(35) Gorman, A. A.; Lovering, G.; Rodgers, M. A. J. *J. Am. Chem. Soc.* **1979**, *101*, 3050−3055.

The entropy difference between **9opn** and **TS10** is positive (10.0 cal/(mol·K)), which means that the second barrier (**9opn** → **11**) becomes larger with increasing temperature. At 0 K, the free energy barrier is negative ($\Delta G^{\ddagger} = -0.4$ kcal/mol) but increases to 1.8 kcal/mol at 298 K. Thus the nature of the O_2 addition reaction changes from concerted nonsynchronous to nonconcerted as the temperature increases.

It is interesting that the energy of concert (the difference between the concerted (**12**) and stepwise stationary points) is larger for addition to 1,3-cyclohexadiene (16.7−6.5 = 10.2 kcal/mol, Figure 2) compared to *cis*-1,3-butadiene[6c] (3.0 kcal/mol). The most likely explanation is the decreased flexibility of the two sp^2 carbons which form C−O bonds in 1,3-cyclohexadiene.

There are two ene reactions. One is a two-step reaction to form 1-hydroperoxy-2,4-cyclohexadiene (**18**), while the other, which forms 1-hydroperoxy-2,5-cyclohexadiene (**5**), is concerted. The two-step reaction to **18** proceeds through intermediate **9** with the second step (**TS17**) involving the abstraction of a methylene hydrogen by the terminal oxygen of the peroxide group (**TS17**). While the activation barrier for the second step is small (10.3 kcal/mol), it is still much larger than closure to the endoperoxide ($\Delta H^{\ddagger} = -0.4$ kcal/mol), which indicates that the latter pathway will prevail.

The reaction to **5** is concerted with an activation barrier of 8.8 kcal/mol. In the transition structure (**TS4**), the C−O bond has formed to a greater extent (1.775 Å) than the nascent O−H bond (1.874 Å). The CASPT2 HOMO/LUMO natural populations indicate significant but not extensive diradical character (1.815/0.208). Comparing **TS4** and **TS8**, the two low-energy transition structures from **1** + $^1O_2$ ($\Delta H^{\ddagger} = 8.8$ and 6.5 kcal/mol, respectively), the entropy difference (5.8 cal/(mol·K)) would favor **TS8** with an increase in temperature, while the dipole moments (3.58 and 2.89 D, respectively) would favor **TS4** in more polar solvents. The predicted solvent effect is consistent with the experimental observations of Griesbeck et al.,[36] who found that the percentage of ene product relative to endo product increased with solvent polarity in the photooxygenation of 2,4-dimethyl-1,3-pentadiene.

Two additional transition structures leading from **9** have been calculated (**TS13** and **TS15**). While both are higher in energy than **TS10**, with appropriate substituents one or both might become low enough to be competitive. **TS13** is the transition structure for closure to the dioxetane **14** ($\Delta H^{\ddagger} = 9.5$ kcal/mol, Figure 2 (4.0 +5.5)) while **TS15** is the transition structure ($\Delta H^{\ddagger} = 24.5$ kcal/mol, Figure 2 (19.0 + 5.5)) for the abstraction of the α-hydrogen by the terminal (distal) oxygen to form 1-hydroperoxy-1,3-cyclohexadiene (**16**).

For the sake of completeness and because formation of dioxetane occurs via a rather low activation barrier, we considered the O−O bond cleavage reaction of **14** (Figure 3). In the transition structure (**TS19**) the O−O bond distance has elongated from 1.489 to 2.031 Å while the C−C distance of the two carbons in the four-membered ring has barely changed (1.530 → 1.546 Å). After the transition structure is passed, the C−C bond begins to cleave giving **20** as the first stable product. Other lower energy conformers of the dialdehyde are possible. While **21** (3.0 kcal/mol lower than **20**) has two imaginary frequencies at the B3LYP/6-31G(d) level, it is probably close to the lowest energy dialdehyde conformer. The activation barrier for O−O bond cleavage in **14** → **21** (15.8 kcal/mol) is similar to the experimental activation barrier[37] for O−O bond cleavage in dioxetane (19−23 kcal/mol) to give two formaldehydes.

(36) Griesbeck, A. G.; Fiege M.; Gudipati, M. S.; Wagner, R. *Eur. J. Org. Chem.* **1998**, 2833−2838.

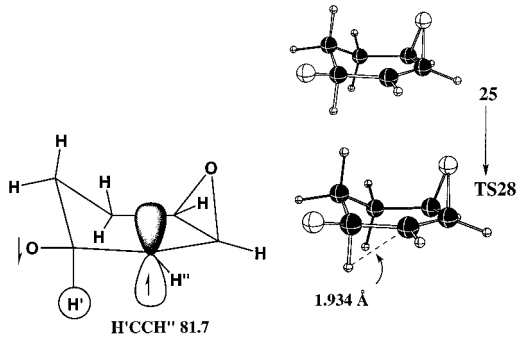

Figure 9. Illustration of the HCCH dihedral angle in **TS28**. Very little activation is required to reach the transition structure **TS28** from **25**.

Reactions of Cyclohexadiene Endoperoxide. The O−O bond in cyclohexadiene endoperoxide **11** cleaves with an activation barrier of 20.5 kcal/mol (**TS22**) to give the diradical **23** (Scheme 5 and Figure 4). The O−O distance increases from 1.481 to 2.331 Å in going from reactant to transition structure, while the diradical character (i.e. CASPT2 HOMO/LUMO population) increases from 1.899/0.090 in **11** to 1.368/0.631 in **TS22**. From **23**, two pathways are considered: C−C bond cleavage to give an acyclic diradical (**TS30**) and intramolecular ring closure to form an epoxide (**TS24**). The first pathway (**TS30**) has a barrier of 16.6 kcal/mol and, rather than giving the expected diradical (**31**), instead cleaves a second C−C bond after the transition structure to form maleic aldehyde plus ethylene. The absence of the diradical **31** on the potential energy surface may be due to the known[38] tendency of DFT to underestimate activation barriers by a few kilocalories per mole. The second pathway (**TS24**) has an activation barrier of only 6.2 kcal/mol and leads to the diradical **25**, where significant unpaired spin density resides on an sp^2 hybridized carbon and on one oxygen atom. From **25**, two low-energy pathways are possible. A second epoxide ring can form (eq 8, **TS26**) with a barrier of 3.1 kcal/mol to give the *syn*-diepoxide, **27**. Alternatively, a hydrogen atom can migrate (eq 9, **TS28**) with a negative activation barrier ($\Delta H^{\ddagger} = -0.7$ kcal/mol) to give the epoxyketone **29**. The prediction that the major product is **29**, not **27**, is consistent with experimental observation.[15] As suggested by Carless et al.,[15] ring closure to give diepoxide **27** is in competition with 1,2-hydrogen shift to give epoxyketone **29** with a difference of 3.8 kcal/mol in activation energies favoring epoxyketone formation. At 298 K, the calculated free energy difference is 3.9 kcal/mol.

The 1,2-hydrogen shift in **TS28** is facilitated by parallel arrangement of a p-orbital on carbon with the adjacent axial C−H bond (Figure 9). The hydrogen shift distances, i.e. C−H···C, and the −HCCH− dihedral angles in **TS28** and **25** are 1.934 Å, 81.7° and 1.994 Å, 82.7°, respectively. It is for this reason that the ratio of diepoxide to epoxyketone is dependent on structural and conformational changes of the endoperoxide, as is known from the literature.[1,15] If the activation energy of the hydrogen shift pathway is increased through the formation of a complex with a catalyst such as CoTPP, it is possible to suppress this pathway completely and only form the diepoxide product.

(37) Adam, W.; Heil, M.; Mosandl, T.; Saha-Möller, C. R. In *Organic Peroxides*; Ando, W., Ed.; Wiley & Sons: Chichester, 1992; p 252.

(38) (a) In a comparison with experiment of 60 barrier heights, DFT gives barrier heights too low by about 3 kcal/mol. See: Lynch, B.; Fast, P. L.; Harris, M.; Truhlar, D. G. *J. Phys. Chem.* **2000**, *104*, 4811−4815. (b) For a possible explanation for why DFT predicts barrier heights too low see: Rassolov, V. A.; Ratner, M. A.; Pople, J. A. *J. Chem. Phys.* **2000**, *112*, 4014−4019.

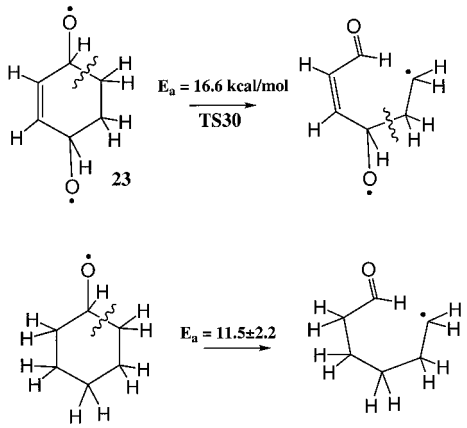

Figure 10. The calculated activation energy for C−C cleavage in **TS30** (16.6 kcal/mol) is compared to the experimental activation energy[41] of C−C bond cleavage in oxycyclohexane (11.5 ± 2.2 kcal/mol).

The calculated activation enthalpy for eq 8 (22.0 kcal/mol) is smaller than the activation enthalpy for other endoperoxides[39] and much smaller than the O−O bond dissociation enthalpies for alkyl peroxides such as CH_3OOCH_3 (38.3 kcal/mol[40]). However, low activation enthalpies are generally observed for saturated endoperoxides in ring systems having strain, which reduces the O−O bond energy.[38c] The activation entropy of O−O clevage in **11** (3.3 cal/(mol·K)) is small and similar to the experimental value for ascoridole (2.6 cal/(mol·K)).[39b]

Thus the products obtained from C−C bond cleavage (**TS30**) appear to be less likely than products from O−O bond scission (**TS24**) since the difference in energy is 10.4 kcal/mol. As a point of comparison, the activation barrier for ring opening in the cyclohexoxy radical is 11.5 ± 2.2 kcal/mol in the gas phase,[41] which is similar to the value of 16.6 kcal/mol for **23** → **TS30** (Figure 10).

While the diradical **31** does not exist on the UB3LYP/6-31G(d) potential energy surface, it does at the UMP2/6-31G(d) level where the C−C bond under discussion has a length of 1.584 Å. An estimate of the UDFT diradical **31** was made by optimizing the structure and fixing the C−C bond to the value calculated at UMP2/6-31G(d) (1.584 Å). From this diradical, four pathways are possible (Figure 5). First, the diradical can fragment to maleic aldehyde plus ethylene. Second, internal addition of oxygen to the radical center can form a substituted oxetane (**31** → **TS32** → **33**). An analogue of this reaction involving CoTPP catalysis with saturated bicyclic endoperoxides has been observed by Balci and Akbulut[17b] (Figure 11).

Third, hydrogen abstraction by oxygen can form the intermediate **35**, which can cyclize to form a OH-derivative of cyclohexenone (**31** → **TS34** → **35** → **TS36** → **37**). Fourth, **31** can cyclize with little or no barrier to form the C_2-symmetry dioxylcyclohexene diradical **38**. If both oxygens cyclize to epoxides (with little or no barrier), then *anti*-diepoxide forms (**31** →→ **38** →→ **39**). Alternatively, hydrogen abstraction by oxygen can also form the OH-derivative of cyclohexenone (**31** →→ **38** → **TS40** → **37**).

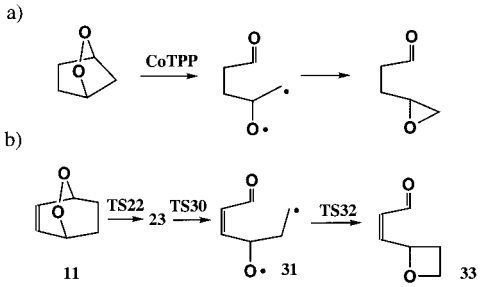

Figure 11. (a) Postulated mechanism for formation of epoxyaldehyde (37% yield) from 2,3-dioxabicyclo[2.2.1]heptane with CoTPP as cataylsis.[17b] (b) Calculated mechanism for formation of lactone from the endoperoxide **11**. In both mechanisms an O−O and C−C bond cleavage has occurred.

The four pathways from **31** have barriers from 0 to 2.6 kcal/mol, which suggests that diradical formation could lead to a number of possible products.

While *syn*-diepoxide can be formed in varying amount from endoperoxides, *anti*-epoxide has not been reported, even as a minor product. In Figure 6, we consider the syn → anti rearrangement. Unlike benzene dioxide, which can undergo facile ring expansion into an eight-membered triene ring,[42] the *syn*-diepoxide **27** undergoes a single C−C bond cleavage to form a diradical intermediate. In **27**, the two epoxide rings are nonequivalent, as there is a cis orientation between one axial methylene hydrogen and oxygen (left-side ring in **27**, Figure 6), while the second epoxide ring (right-side ring in **27**) has a trans relationship with the axial hydrogen of the methylene group. As a consequence, there are two diradical conformers (**42** and **44**) which differ in energy by 2.6 kcal/mol. Intermediate **42** can be formed with an activation barrier of 36.6 kcal/mol and a reverse barrier of 11.4 kcal/mol. Optical activity of a labeled diepoxide is lost when the two intermediates are equilibrated via **TS43** ($\Delta H^{\ddagger}$ = 5.2 kcal/mol). The syn−anti rearrangement takes place via **TS45** or **TS47**, which are 17.7 and 19.9 kcal/mol above **42** and **44**, respectively. Thus the lowest path to *anti*-diepoxide is **27** → **TS41** → **42** → **TS45** →**46**. The *anti*-diepoxide conformer **46**, which is 3.7 kcal/mol higher than conformer **39**, can rearrange to **39** by a simple ring inversion (not calculated). Our calculations predict that optically active *syn*-diepoxide will racemize with a barrier of 36.6 kcal/mol and will rearrange to *anti*-diepoxide with a barrier of 42.9 kcal/mol and an exothermicity of 3.8 kcal/mol.

Vertical Excitation Energies of Endoperoxides. The photochemical reaction of anthracene-9,10-endoperoxide (and derivatives) gives different products depending on the wavelength of light used.[19−22] At wavelengths longer than about 280 nm, rearrangement involving O−O bond cleavage takes place, while at wavelengths shorter than about 280 nm, molecular O_2 cleaves predominately. The current interpretation of these phenomena postulates that reversion takes place from a S_1 state ($\pi^* \rightarrow \pi^*$ excitation), while the O−O fragmentation takes place from a S_2 state ($\pi^* \rightarrow \sigma^*$ excitation). However, Klein et al.[19] have questioned this interpretation. On the basis of INDO/S and CNDO/S calculations of several endoperoxides, they conclude that rearrangement takes place from excitation into the triplet manifold since the calculated lowest S_1 state has $\pi^*\pi^*$ character, which would more likely lead to cycloreversion. The excitation energies for the two lowest triplet excited states and several singlet excited states are given in Table 3 at the TD-B3LYP/6-31+G(d) level for cyclohexadiene and cyclopentadiene en-

(39) (a) The experimental activation barriers for thermolysis are $\Delta H^{\ddagger}$ = 31.4 kcal/mol and $\Delta S^{\ddagger}$ = 2.6 eu for ascoridole[38b] and $\Delta H^{\ddagger}$ = 33.1 kcal/mol and $\Delta S^{\ddagger}$ = 3.0 eu for cyclohexane endoperoxide.[38c] (b) Boche, J.; Runquist, O. *J. Org. Chem.* **1968**, *33*, 4285−4286. (c) Coughlin, D. J.; Salomon, R. G. *J. Am. Chem. Soc.* **1979**, *101*, 2761−2763.

(40) Atkinson, R.; Baulch, D. L.; Hampson, R. A., Jr.; Cox, R. A.; Kerr, J. A.; Rossi, M. J.; Troe, J. *J. Phys. Ref. Data* **2000**, *29*, 167−266 (see pp 264−266).

(41) Orlando, J. J.; Iraci, L. T.; Tyndall, G. S. *J. Phys. Chem. A* **2000**, *104*, 5072−5079.

(42) Boyd, D. R.; Sharma, N. D.; O'Dowd, C. R.; Hempenstall, F. *Chem. Commun.* **2000**, 2151−2152.

Table 3. Computed Excitation Energies (nm) and Oscillator Strengths for Singlet and Triplet States of Cyclopentadiene and Cyclohexadiene Endoperoxides with TD-B3LYP/6-31+G(d)[a]

state	excited energy (nm)[b]	oscillator strength	description
	cyclopentadiene endoperoxide		
S0 (^{1}A′)	0	0	
T1 (^{3}A′)	379 (179)	0	
T2 (^{3}A″)	333 (377)	0	
S1 (^{1}A′)	290 (179)	0.002	$(\pi^*_{OO}) \rightarrow (\pi^*_{CC} + \sigma^*_{OO})$
S2 (^{1}A′)	248 (146)	0.006	$(\pi^*_{OO}) \rightarrow (\sigma^*_{OO} + \pi^*_{CC})$
S3 (^{1}A″)	215 (213)	0.002	$(\pi^*_{OO}) \rightarrow$ (mixed)
S4 (^{1}A″)	209 (156)	0.036	$(\pi_{CC}) \rightarrow (\pi^*_{CC})$
	cyclohexadiene endoperoxide (**11**)		
S0 (^{1}A′)	0	0	
T1 (^{3}A′)	390	0	
T2 (^{3}A″)	317	0	
S1 (^{1}A′)	294	0.001	$(\pi^*_{OO}) \rightarrow (\pi^*_{CC} + \sigma^*_{OO})$
S2 (^{1}A′)	257	0.003	$(\pi^*_{OO}) \rightarrow (\sigma^*_{OO} + \pi^*_{CC})$
S3 (^{1}A″)	229	0.001	$(\pi^*_{OO}) \rightarrow$ (mixed)
S4 (^{1}A′)	207	0.010	$(\pi^*_{OO}) \rightarrow$ (mixed)
S5 (^{1}A″)	202	0.047	$(\pi_{cc}) \rightarrow (\pi^*_{cc})$

[a] Only the two lowest energy triplet states are listed. [b] Values in parentheses are the excitation energies calculated at the CNDO-SDCI level (ref 19a).

doperoxide. The TD-DFT results (Table 3) for cyclopentadiene endoperoxide differ significantly from the CNDO-SDCI results of Klein et al.[19a] At the TD-DFT level, the dominant configuration of the S_1 excited state (290 nm) involves excitation from the HOMO (π^*_{OO}) into the LUMO (π^*_{CC}) with a smaller contribution from a HOMO (π^*_{OO}) → LUMO-1 (σ^*_{OO}) excitation. Excitation into this state would not weaken the O−O bond and may lead to cycloreversion products. The S_2 state (248 nm) involves a dominant HOMO (π^*_{OO}) → LUMO-1 (σ^*_{OO}) excitation with a smaller contribution from HOMO (π^*_{OO}) → LUMO (π^*_{CC}). Thus, the *second* excited state leads to a much weakened O−O bond, which would favor rearrangement. The results for cyclohexadiene endoperoxide are essentially the same, as expected. The S_1 state (294 nm) and S_2 state (257 nm) occur at slightly longer wavelength compared to cyclopentadiene endoperoxide (290 and 248 nm). Our results favor the original interpretation by Kearns.[20]

Conclusions

A comprehensive study of singlet oxygen addition to 1,3-cyclohexadiene at the CASPT2(12e,10o)/6-31G(d)//B3LYP/6-31G(d)+ZPC level has revealed a number of interesting features. The cyclohexadiene endoperoxide is formed with an activation barrier of 6.5 kcal/mol in a reaction that is concerted but very nonsynchronous. The reaction is two-step at the DFT level, but the barrier of the second step disappears at the CASPT2 level. As the temperature increases, the reaction is predicted to become more nonconcerted with a free energy barrier of the second step of 1.8 kcal/mol at 298 K. The ene reaction is predicted to be concerted with a barrier of 8.8 kcal/mol, only 2.3 kcal/mol higher than the barrier for endoperoxide formation.

The endoperoxide **11** is predicted to form two main products, epoxyketone **29** and diepoxide **27**, in agreement with experimental observations. The O−O bond cleaves with a 20.5 kcal/mol barrier to form the first diradical intermediate (**23**), and then passes a 6.2 kcal/mol barrier to form a second diradical intermediate (**25**). From the second intermediate a −0.7 kcal/mol barrier leads to **29** and a 3.1 kcal/mol barrier leads to **27**. The syn−anti rearrangement was studied for diepoxide (**27**). It is predicted that optically active *syn*-diepoxide will racemize with a barrier of 36.6 kcal/mol and undergo syn → anti arrangement with a barrier of 42.9 kcal/mol.

Finally, excitation energies calculated at the TD-B3LYP/6-31+G(d) level for endoperoxides of cyclopentadiene and cyclohexadiene indicate that photorearrangement should take place from $S_0 \rightarrow S_1$ excitation and photoreversion should take place from $S_0 \rightarrow S_2$ excitation.

Acknowledgment. Computer time was provided by the Alabama Supercomputer Network and Maui High Performance Computer Center. M.L.M. would like to thank Sun Microsystems Computer Corporation for the award of an Academic Equipment Grant. F.S. thanks Professor Metin Balci for his support and valuable insight and also the NATO Science Fellowship Program administered by The Scientific and Technical Research Council of Turkey (TUBITAK) for a grant and Professor Hamdullah Kilic for helpful discussions.

Supporting Information Available: Tables of the total energies (hartree) at B3LYP/6-31G(d), CASSCF(12e,10o)//6-31G(d), and CASPT2(12e,10o)//6-31G(d) levels and thermodynamic parameters of stationary points at the B3LYP/6-31G(d) level and Cartesian coordinates for relevant structures optimized at the B3LYP/6-31G(d) level (/PDF). This material is available free of charge via the Internet at http://pubs.acs.org.

JA010138X